



# Low-temperature prepared highly effective ferric hydroxide supported gold catalysts for carbon monoxide selective oxidation in the presence of hydrogen<sup>☆</sup>

Botao Qiao<sup>a,b</sup>, Juan Zhang<sup>a,b</sup>, Lequan Liu<sup>a,b</sup>, Youquan Deng<sup>a,b,\*</sup>

<sup>a</sup> Center for Green Chemistry and Catalysis, Lanzhou Institute of Chemical Physics, Chinese Academy of Sciences, Lanzhou 730000, China

<sup>b</sup> Graduate University of Chinese Academy of Sciences, Beijing 100039, China

## ARTICLE INFO

### Article history:

Received 16 October 2007

Received in revised form 21 January 2008

Accepted 13 February 2008

Available online 10 March 2008

### Keywords:

Gold catalyst

CO selective oxidation

Preparation

Uncalcined

Low-temperature

## ABSTRACT

Ferric hydroxide supported Au catalysts prepared with co-precipitation method at room temperature without any heat treatment hereafter exhibited high catalytic activity and selectivity for CO oxidation in air and CO selective oxidation in the presence of H<sub>2</sub>. With calcination temperature rising, both activity and selectivity decreased. X-ray Photoelectron Spectra (XPS) indicated that Au existed as Au<sup>0</sup> and Au<sup>+</sup> in the catalyst without heat treatment and even after being calcined at 200 °C, while after being calcined at 400 °C, Au existed as Au<sup>0</sup> completely. X-ray Diffraction (XRD) and High Resolution Transmission Electron Microscopic (HRTEM) investigations indicated that both the supports and Au species were highly dispersed as nano or sub-nano particles even after being calcined at 200 °C, but after being calcined at 400 °C the supports transformed to crystal Fe<sub>2</sub>O<sub>3</sub> with typical diameter of 30 nm and Au species aggregated to nano-particles with typical diameter of 2–4 nm. HRTEM investigations also suggested that the supports calcined at 200 °C were composed of amorphous ferric hydroxide and crystal ferric oxide. Results of computer simulation (CS) showed that O<sub>2</sub> was adsorbed on Au crystal cell and then were activated, which should be the key factor for the subsequent reaction. It also suggested that O<sub>2</sub> species were more easily adsorbed on Au<sup>+</sup> than on Au<sup>0</sup>, indicating that higher positive charge of the Au species possessed the higher activity for CO oxidation.

© 2008 Elsevier B.V. All rights reserved.

## 1. Introduction

Because of its great importance for practical applications, considerable effort has been applied to develop suitable catalysts for the selective oxidations of CO in the presence of H<sub>2</sub>. The most commonly used catalysts are supported noble metal catalysts, such as supported Pt, Ru, Rh, Pt-Pd bimetal, etc. [1–7]. However, these catalysts are usually not very active for CO oxidations and it was found that, at lower temperatures, the CO oxidation was rather slow due to inhibition of oxygen adsorption [1], while at temperature above 200–250 °C the selectivity decreased because thermal desorption of CO enables H<sub>2</sub> oxidations. Recently, Tanaka et al. found that Pt/Al<sub>2</sub>O<sub>3</sub> and Pt/CeO<sub>2</sub> [8] and Pt/TiO<sub>2</sub> [9] catalysts could be highly activated by depositing FeO<sub>x</sub> and could be effective catalysts for CO selective oxidations, while they deduced that the

deposited FeO<sub>x</sub> was activated by the Pt and the FeO<sub>x</sub> was responsible for the selective oxidation of CO.

Highly dispersed gold on suitable supports is highly active for low-temperature CO oxidation [10,11] and less active for H<sub>2</sub> oxidation [11,12]. Furthermore, the catalytic activity of Au is enhanced by moisture [13] and almost insensitive to CO<sub>2</sub> [14], indicating that supported gold catalysts may be suitable for selective oxidizing CO in a H<sub>2</sub> environment. Since Haruta demonstrated firstly that the supported gold catalysts could be effective for CO selective oxidations in the presence of H<sub>2</sub> [12,15], several gold catalysts [16–18] supported by γ-Al<sub>2</sub>O<sub>3</sub> such as Au/Al<sub>2</sub>O<sub>3</sub>, Au/MnO<sub>x</sub>/Al<sub>2</sub>O<sub>3</sub>, and Au/MgO/Al<sub>2</sub>O<sub>3</sub>, etc., were investigated. It was found that, in Au/Al<sub>2</sub>O<sub>3</sub> catalysts system, the presence of Mg citrate in the preparation solution had a significant effect on the properties of the catalyst. Catalysts prepared without citrate contained larger Au particles and were less active and less selective for CO oxidation [16]. Nieuwenhuys and Grisel showed that the presence of MgO enabled the preparation of small, stable Au particles on γ-Al<sub>2</sub>O<sub>3</sub> with high surface area and, in this way, improved both low-temperature CO and H<sub>2</sub> oxidation compared to Au/Al<sub>2</sub>O<sub>3</sub> [17]. Addition of MnO<sub>x</sub> and FeO<sub>x</sub> to Au/MgO/Al<sub>2</sub>O<sub>3</sub> further enhances low-temperature CO oxidation with improved CO<sub>2</sub>

<sup>☆</sup> This work was financially supported by The National Natural Science Foundation of China (No. 20773146).

\* Corresponding author at: Center for Green Chemistry and Catalysis, Lanzhou Institute of Chemical Physics, Chinese Academy of Sciences, Lanzhou 730000, China. Tel.: +86 931 4968116; fax: +86 931 4968116.

E-mail address: [ydeng@lzb.ac.cn](mailto:ydeng@lzb.ac.cn) (Y. Deng).

selectivity. The increase in CO oxidation activity is attributed to the implementation of new routes for supplying active oxygen, e.g. via lattice oxygen. The better CO<sub>2</sub> selectivity also probably results from suppression of H<sub>2</sub> oxidation at low temperatures [18].

More recently, Wan and co-workers found that Au/TiO<sub>2</sub> catalyst had a good performance for CO oxidations in the presence of H<sub>2</sub> that the catalysts could convert about 100% CO with a 80% selectivity towards CO<sub>2</sub> at 25 °C [19]. Rousset and co-workers reported that Au/ZrO<sub>2</sub> catalyst obtained simply by oxidation of Au<sub>0.5</sub>Zr<sub>0.5</sub> alloy at room temperature had a better performance for CO selective oxidation in the presence of H<sub>2</sub> at 100 °C, while this catalyst had a much higher gold content of 61.5 wt% [20]. Corma and co-workers reported a nano-crystalline CeO<sub>2</sub>-supported Au catalyst that gave appreciable selectivity at 60 °C for a dry CO–H<sub>2</sub> [21]. Au/Fe<sub>2</sub>O<sub>3</sub> catalysts have also been studied [22,23]. Behm and co-workers have investigated the influence of H<sub>2</sub>O and CO<sub>2</sub> on CO selective oxidations over Au/Fe<sub>2</sub>O<sub>3</sub> catalysts calcined at 400 °C [22]. Hutchings and co-workers reported Au/Fe<sub>2</sub>O<sub>3</sub> catalysts prepared using a two-stage calcination procedure and this catalyst had a good performance in fuel cells [23].

While, the catalysts mentioned above all needed calcination at elevated temperatures in the preparation process, which was a process of time and energy consuming and releasing polluted gases, such as NO<sub>x</sub>, HCl, CO<sub>2</sub>, etc. In our previous communication [24], we have reported an Au/Fe(OH)<sub>x</sub> catalyst prepared with a simple and environment friendly co-precipitated method, which was very effective for CO oxidation and selective oxidation of CO in the presence of H<sub>2</sub>. Herein, we extended the reaction and characterization data greatly and presented a relatively systematic investigation of this catalyst.

## 2. Experimental

### 2.1. Catalysts preparation

All chemicals used in the experiments were of analytical grade, and were used without further purification. The catalysts with varied gold loadings were prepared by co-precipitation. Aqueous solution of HAuCl<sub>4</sub> (0.24 mol/L) and Fe(NO<sub>3</sub>)<sub>3</sub> (1 mol/L) were mixed and added dropwise into 10 wt% aqueous solution of NaCO<sub>3</sub> at room temperature with vigorous stirring, final pH was adjusted to about 8. After 3 h stirring and aging, the resulted precipitate was washed for several times with distilled water until chloride could not be detected by 0.1 mol/L AgNO<sub>3</sub>, then filtrated and dried at room temperature (about 25 °C) and atmospheric pressure for 24 h. The resulted solids used as catalysts directly were denoted as Au/Fe-UC. For comparison, the catalysts Au/Fe-UC were further calcined in air at 200 °C (denoted as Au/Fe-C2) and 400 °C (Au/Fe-C4), respectively. It should be noted that different calcination temperatures resulted in different gold loadings although the same amount of gold precursor and aqueous solution of Fe(NO<sub>3</sub>)<sub>3</sub> were used.

### 2.2. Catalysts characterization

Au loadings in the catalyst samples were measured using a 3520 ICP AES instrument of AR Co., USA. Due to water losing and support transforming from hydroxide to oxide, it should be noted that different Au loadings were resulted between uncalcined and calcined samples, although the same quantity of gold precursors were initially used.

N<sub>2</sub> adsorption measurements were performed on a Micromeritics ASAP 2020 instrument at 77 K and the surface area of the support was obtained by the Brunauer–Emmett–Teller (BET) method. It must be pointed that the Au/Fe-UC catalyst samples were outgassed to 0.1 Pa at 50 °C so as to assure no changes in the support structure. The other catalysts, Au/Fe-C2 and Au/Fe-C4, were outgassed to 0.1 Pa at 200 °C.

The X-ray Diffraction (XRD) measurements for the structure determination were carried on a Siemens D/max-RB powder X-ray Diffract meter. Diffraction patterns were recorded with Cu Kα radiation (40 mA, 40 kV) over a 2θ-range of 15° to 75° and a position-sensitive detector using a step size of 0.01° and a step time of 0.15 s.

The X-ray Photoelectron Spectroscopy (XPS) analyses were performed on a VG ESCALAB 210 instrument. Mg Kα radiation at a pass energy of 150 eV at an energy scale calibrated versus C 1s peak at 285.1 eV arising from adventitious carbon were used. The surface composition of the samples was determined from the peak areas of the corresponding lines using a Shirley-type background and empirical cross-section factors for XPS. The sample powders were palletized and then mounted on double-side adhesive tape. The pressure in the analysis chamber was in the range of 10<sup>−9</sup> Torr during data collection and the sample has been in such a low pressure for 24 h without heating before analyzed.

High Resolution Transmission Electron Microscopic (HRTEM) investigations were carried out using a JEOL JEM-2010 Electron Microscope. The powder of Au catalysts was suspended in toluene with an ultrasonic dispersion for 5–10 min and then the resulted solution was dropped on a copper grid.

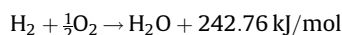
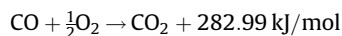
Fourier Transform Infrared Spectroscopy (FT-IR) studies were performed with a Nicolet 5700 FR-IR with corresponding OMNIC software at room temperature and atmospheric pressure.

Computer simulations (CS) of O<sub>2</sub> adsorbed on Au(1 0 0) with or without electric charge were performed with DMol<sup>3</sup> of Materials Studio (Accelrys) based on the Density Functional Theory (DFT).

### 2.3. Catalytic activity measurements

Catalytic activity measurements were carried out in a micro fixed-bed reactor, with 60 mg catalyst sieved to 60–80 mesh. The micro fixed-bed reactor was placed in a furnace with temperature programmed and the precision of temperature rising can be controlled in 0.1 °C. When activity test was carried out below room temperature, dry ice was employed and ethanol was used to adjust various temperatures. The feed gases for the oxidation were 1 vol% CO with air balanced and 1 vol% H<sub>2</sub> with air balanced. For the selective oxidation, the gas were 1 vol% CO, 1 vol% H<sub>2</sub> and 4 vol% O<sub>2</sub> balanced with Argon. Another gas for selective oxidation was used with composition of 1 vol% CO, 4 vol% O<sub>2</sub> and 50% H<sub>2</sub> balanced with Argon. Also, in order to make an comparison with the results in the literatures, the gas with composition of 1 vol% CO, 1% H<sub>2</sub> and 0.5 vol% O<sub>2</sub> was used. The flow rate was 20 ml/min, which resulted in a space velocity of 20,000 h<sup>−1</sup> ml/g-cat. The concentration of CO, H<sub>2</sub> and O<sub>2</sub> in the effluent gas was on-line analyzed by a Angilent 1790T gas chromatograph with a molecular sieve 5 A plot column.

The reaction were:



CO selectivity was calculated according to the following formula:

$$S_{\text{CO}}(\%) = \frac{1\% \times C_{\text{CO}}}{1\% \times C_{\text{CO}} + 1\%(50\%) \times C_{\text{H}_2}} \times 100\%$$

S<sub>CO</sub> means the selectivity of CO, C<sub>CO</sub> means the conversion of CO, C<sub>H<sub>2</sub></sub> means the conversion of H<sub>2</sub>.

## 3. Results

### 3.1. Catalytic activity measurements

Complete CO oxidations in air at ca. 8 °C, 22 °C and 87 °C were observed over 0.76 wt% Au/Fe-UC, 1.1 wt% Au/Fe-C2 and 1.5 wt%

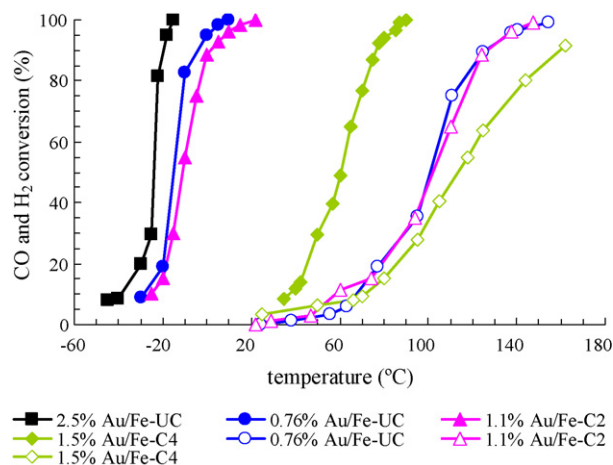


**Fig. 1.** Conversion of CO (solid symbol) in 1 vol% CO in air and H<sub>2</sub> (open symbol) in 1 vol% H<sub>2</sub> in air over different catalysts respectively.

Au/Fe-C4, respectively, Fig. 1, indicating that CO oxidation was sensitive to the heat treatments, and calcinations at elevated temperatures were detrimental to the catalytic performance. Therefore, Au/Fe-UC was the best catalyst for CO oxidation although its Au loading was the lowest. As expected, when the Au loading was further increased from 0.76 to 2.5 wt%, the catalytic activity could be markedly increased, i.e. complete CO oxidation in air at ca.  $-15^{\circ}\text{C}$  was achieved. In comparison with CO oxidation, oxidations of H<sub>2</sub> were much less sensitive to the heat treatment and occurred above ca.  $25^{\circ}\text{C}$  over all the three catalysts. Since the chemical composition, structure and chemical state of Au/Fe-UC are completely different from that of Au/Fe-C4, it could be conjectured that CO oxidation was highly sensitive to such changes, while the active species of gold for H<sub>2</sub> oxidation were already formed before any heating treatments and did almost not change when they were further subjected to calcination at elevated temperatures. It is worth noting that there is about  $20^{\circ}\text{C}$  gap between the temperatures of complete CO oxidation and the occurrence of H<sub>2</sub> oxidation for Au/Fe-UC. This may imply that Au/Fe-UC could be an ideal catalyst for the selective CO oxidation in the presence of H<sub>2</sub> at lower temperatures.

Previously reported work [13] indicated that small amount of water in the feed gas might be favorable for the CO total oxidation at lower temperatures. Since calcinations at elevated temperature were omitted, Au/Fe-UC catalysts should contain relatively higher content of water. However, it was found that the catalytic activity of Au/Fe-UC catalysts would not almost decrease when they were dried at  $100^{\circ}\text{C}$  for several hours to remove the water completely,

indicating that higher activity of Au/Fe-UC catalysts may less related to the relatively higher content of water in the catalysts.

When the same catalysts as mentioned above were exposed to the mixture gas of 1 vol% H<sub>2</sub>, 1 vol% CO and 4 vol% O<sub>2</sub>, different behavior of catalytic oxidation over them were exhibited, Fig. 2(a) and (b). The lowest temperature for CO totally oxidation increased greatly and relatively high H<sub>2</sub> conversion occurred before all CO could be oxidized completely (ca. 4–30% H<sub>2</sub> conversion), indicating that highly selective CO oxidation in the presence of H<sub>2</sub> over Au/Fe-C4 catalyst was impossible (selectivity of 93–77%, Fig. 2(b)). CO oxidations were also slightly affected by H<sub>2</sub> over Au/Fe-C2 and the temperature at which CO was completely removed, i.e. ca.  $30^{\circ}\text{C}$ , was high enough to cause detectable oxidation of H<sub>2</sub> (ca. 3–6% H<sub>2</sub> conversion and the corresponding selectivity of 96–90%). As for Au/Fe-UC, conversion of CO oxidation as function of temperature was almost unchanged in comparison with the CO oxidation in the absence of H<sub>2</sub>, i.e. the existence of H<sub>2</sub> did not affect the CO oxidation. CO could completely be oxidized at ca.  $10^{\circ}\text{C}$ , while oxidation of H<sub>2</sub> was not detectable at this temperature, i.e. the O<sub>2</sub> selectivity for CO oxidation approached to 100%.

It is worthy to note that, when Au/Fe-UC catalysts with lower gold loadings were employed, the temperatures at which CO was totally removed and H<sub>2</sub> oxidation was initiated were increased simultaneously, suggesting that the temperature for selective CO oxidation in the presence of H<sub>2</sub> could be set by adjusting the gold loadings without decrease of the selectivity of CO oxidation. As shown in Fig. 3(a) and (b), over 0.28 wt% Au/Fe-UC and 0.16 wt% Au/Fe-UC catalysts, CO were completely oxidized at  $38^{\circ}\text{C}$  and  $53^{\circ}\text{C}$ , respectively, while the H<sub>2</sub> oxidations over them occurred at  $57^{\circ}\text{C}$  and  $60^{\circ}\text{C}$  (conversion of 0.4%) respectively. While over 0.06 wt% Au/Fe-UC catalyst, at the temperature that CO were completely oxidized about 2% H<sub>2</sub> conversion was detected (which resulting a selectivity of 98%), indicating that the temperature for CO oxidation in the presence of H<sub>2</sub> could only be set in a certain range by adjusting the gold loadings.

To investigate the competitive ability of CO oxidations and H<sub>2</sub> oxidations, H<sub>2</sub> concentration in the mixture gas was greatly increased to 50% and the reaction temperature was increased greatly from room temperature. Conversion of CO oxidation was restrained by H<sub>2</sub> over 0.76 wt% Au/Fe-UC and the temperature of CO total conversion increased to  $45^{\circ}\text{C}$  because the concentration of H<sub>2</sub> in feed gas was greatly increased. And at this temperature, there was ca. 2% H<sub>2</sub> conversion detected. Furthermore, CO oxidations were further inhibited over Au/Fe-C2 and Au/Fe-C4 in comparison with that in mixture of 1 vol% H<sub>2</sub>, 1 vol% CO and 4 vol% O<sub>2</sub> in Argon. However, even if reaction temperature increased to the high temperature of  $220^{\circ}\text{C}$ , conversion of CO decreased unremarkably (ca. 90%, 85% and 78% conversion over

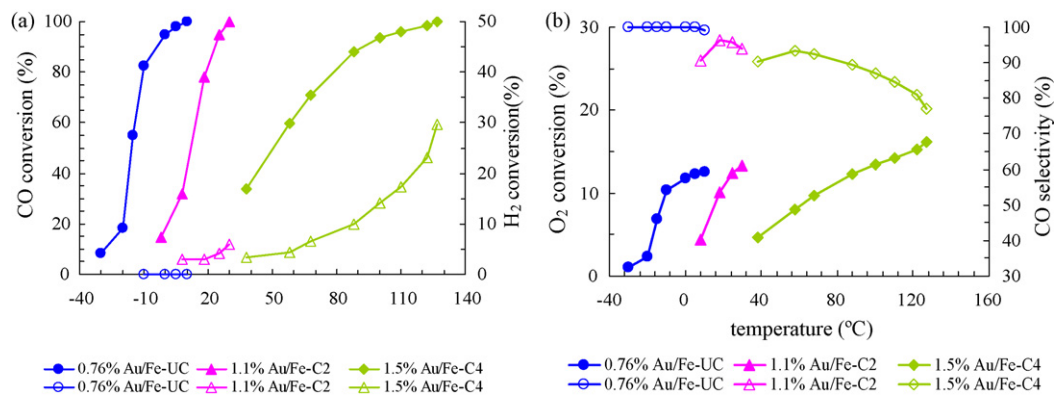


**Fig. 2.** (a) Conversion of CO (solid symbol) and H<sub>2</sub> (open symbol) in CO + H<sub>2</sub> mixture gas (1 vol% H<sub>2</sub>) and (b) the corresponding O<sub>2</sub> conversion (solid symbol) and CO selectivity (open symbol) over different catalysts.

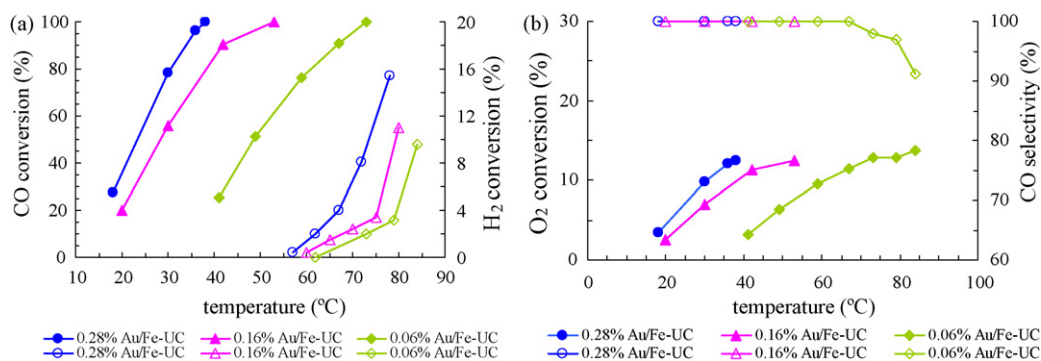


**Fig. 3.** (a) Conversion of CO (solid symbol) and H<sub>2</sub> (open symbol) in CO + H<sub>2</sub> mixture gas (1 vol% H<sub>2</sub>) and (b) the corresponding O<sub>2</sub> conversion (solid symbol) and CO selectivity (open symbol) over different catalysts with lower Au loadings.

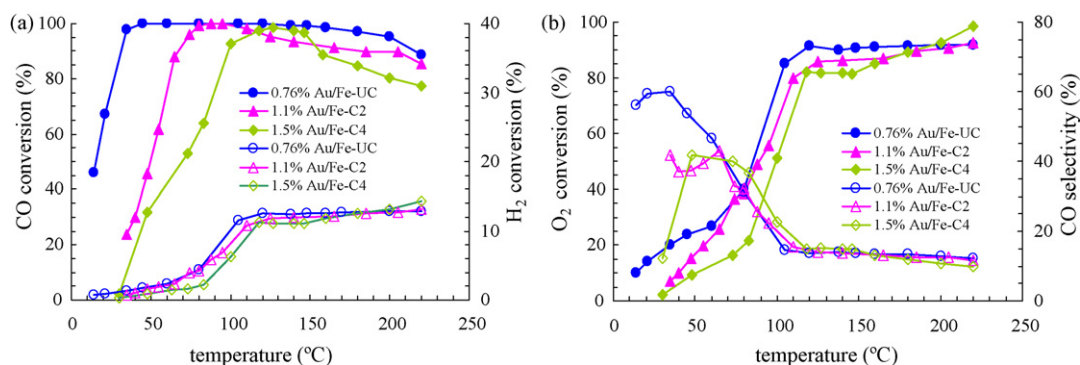


**Fig. 4.** (a) conversion of CO (solid symbol) and H<sub>2</sub> (open symbol) in CO + H<sub>2</sub> mixture gas (50 vol% of H<sub>2</sub>) and (b) the corresponding O<sub>2</sub> conversion (solid symbol) and CO selectivity (open symbol) over different catalysts.

0.76 wt% Au/Fe-UC, 1.1 wt% Au/Fe-C2 and 1.5 wt% Au/Fe-C4 at 220 °C, respectively), indicating that over these catalysts, CO had better competitive ability of consuming O<sub>2</sub> than H<sub>2</sub> even at higher temperatures and in excessive H<sub>2</sub>, especially over Au/Fe-UC catalyst (Fig. 4).

In addition, mixture gas containing less oxygen (1 vol% CO, 1 vol% H<sub>2</sub> and 0.5 vol% O<sub>2</sub>) were investigated, Fig. 5. It can be seen that CO could not be oxidized completely even at about 90 °C over all three catalysts. While, the conversion of CO is still decreased with the increase of calcination temperatures at any reaction temperatures. Further more, the conversion of H<sub>2</sub> is lower than 6% even at about 90 °C, which results in a relatively higher selectivity at about 90 °C.

Also, the stability of catalytic activities of 0.76 wt% Au/Fe-UC and 1.1 wt% Au/Fe-C2 for CO oxidation in air were tested at 30 °C, Fig. 6. The total conversion of CO to CO<sub>2</sub> over 0.76 wt% Au/Fe-UC

could be maintained for about 28 h, and 90% of CO conversion could be further maintained for about 40 h. Over 1.1 wt% Au/Fe-C2, the total conversion of CO to CO<sub>2</sub> could be maintained for about 32 h, slightly longer than over 0.76 wt% Au/Fe-UC, while 90% of CO conversion could only be further maintained for about 25 h, much shorter than over 0.76 wt% Au/Fe-UC. Moreover, when 0.76 wt% Au/Fe-UC catalyst was exposed to 1 vol% CO in air for 120 h, there were still a relatively high CO conversion (75%) while when 1.1 wt% Au/Fe-C2 catalyst was exposed to 1 vol% CO for 90 h the conversion of CO decreased to lower than 50%. The stability of catalytic activities of 0.76 wt% Au/Fe-UC for CO oxidation in mixture of 1 vol% H<sub>2</sub>, 1 vol% CO and 4 vol% O<sub>2</sub> was also tested. The total conversion of CO to CO<sub>2</sub> could only be maintained for 15 h and 80% of CO conversion could be further maintained only for 16 h, indicating that the stability of 0.76 wt% Au/Fe-UC decreased remarkably in 1 vol% H<sub>2</sub>, 1 vol% CO and 4 vol% O<sub>2</sub> mixture gas.

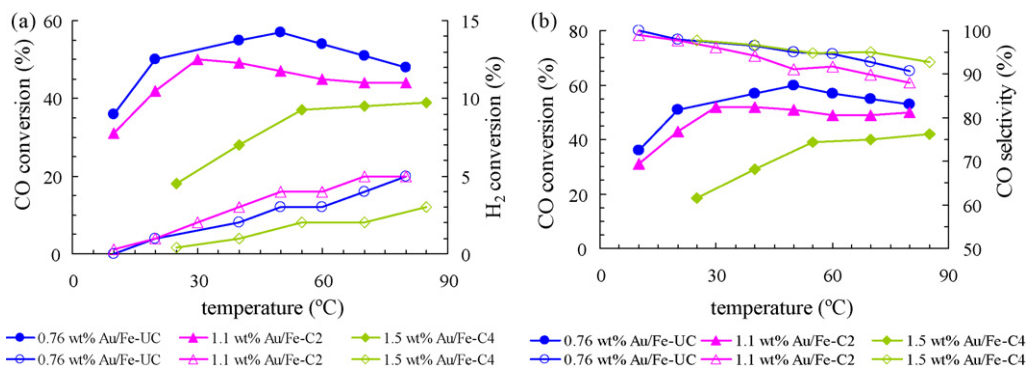


**Fig. 5.** (a) Conversion of CO (solid symbol) and H<sub>2</sub> (open symbol) in CO + H<sub>2</sub> mixture gas (1 vol% CO, 1 vol% H<sub>2</sub> and 0.5 vol% of O<sub>2</sub>) and (b) the corresponding O<sub>2</sub> conversion (solid symbol) and CO selectivity (open symbol) over different catalysts.

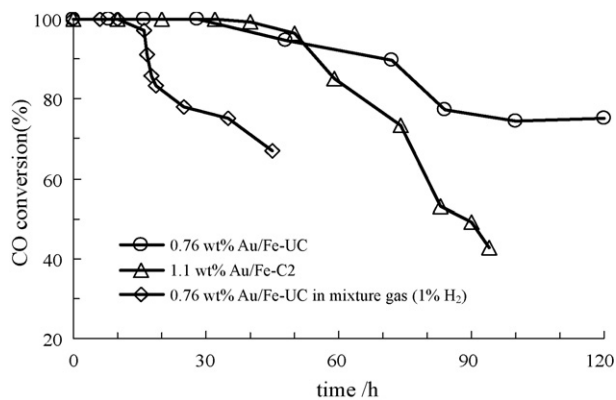


Fig. 6. Stability test of catalytic activity for CO oxidations over supported Au catalyst at 30 °C in different gas and different catalysts.

### 3.2. Catalysts characterization

Results of gold loadings, BET surface areas and XPS of the prepared catalysts are listed in Table 1. Gold loadings, as mentioned above, although the same amount of gold precursor and aqueous solution of  $\text{Fe}(\text{NO}_3)_3$  were used, were increased after being calcined at elevated temperature and this should be related to the losing of adsorbed water and the transformation of ferric hydroxide into metal-oxide. BET adsorption measurement showed that the surface areas decreased greatly with increasing calcinations temperatures. Au/Fe-UC and Au/Fe-C2 had larger BET surfaces which were about 15 and 10 times of that of the Au/Fe-C4 catalyst had. XPS analyses indicated that the surface chemical states of Au existed as  $\text{Au}^0$  (B.E.  $4f_{7/2}$  = 84.2 eV) and  $\text{Au}^+$  (B.E.  $4f_{7/2}$  = 87.7 eV) over 2.5 wt% Au/Fe-UC and the area ratio of  $\text{Au}^+/\text{Au}^0$  was 0.65, Table 1 and Fig. 7. After being calcined at 200 °C, Au still existed as  $\text{Au}^0$  (B.E.  $4f_{7/2}$  = 84.2 eV) and  $\text{Au}^+$  (B.E.  $4f_{7/2}$  = 87.9 eV), while the area ratio of  $\text{Au}^+/\text{Au}^0$  decreased to 0.33. After being calcined at 400 °C, Au species changed to metal completely (B.E.  $4f_{7/2}$  = 83.8 eV). As expected, little  $\text{Cl}^-$  and nitrate species could be observed on the Au/Fe-UC catalyst surface and the nitrate species could be removed after the catalyst were calcined at 200 °C or 400 °C. The contained nitrate species may be one reason that the uncalcined catalysts had higher activity since Hutchings and co-workers found that the nitrate could promote the activity of supported gold catalysts [25]. It should be noted that calcination at elevated temperature could reduce the content of residual  $\text{Cl}^-$ , but  $\text{Cl}^-$  could not be removed completely.

XRD analyses showed that there was no detectable crystallite formation of ferric oxide or hydroxide over 2.5 wt% Au/Fe-UC and 2.9 wt% Au/Fe-C2 catalysts, Fig. 8, indicating that the supports were amorphous even being calcined at 200 °C. When 2.5 wt% Au/Fe-UC catalyst was calcined at 400 °C, typical crystallite of  $\alpha$ - $\text{Fe}_2\text{O}_3$  could be observed, indicating that the supports had transformed from amorphous ferric hydroxide into  $\text{Fe}_2\text{O}_3$ . Also, there was no detectable crystallite formation of Au species over 2.5 wt% Au/Fe-UC since Au species should be highly dispersed without calcinations [26]. While over 3.3 wt% Au/Fe-C4 XRD, peak

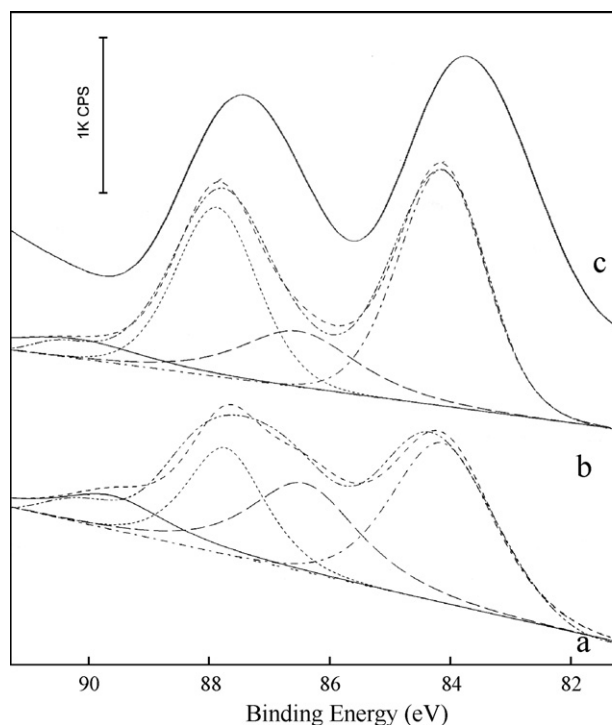


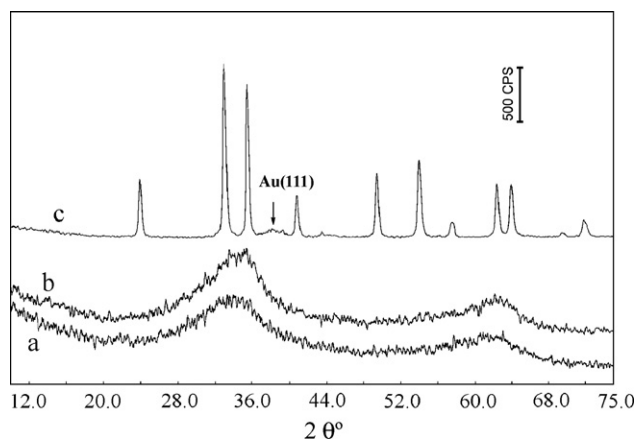
Fig. 7. XPS spectra of different supported Au catalysts, (a) 2.5 wt% Au/Fe-UC, (b) 2.9 wt% Au/Fe-C2 and (c) 3.3 wt% Au/Fe-C4.

of Au (1 1 1) ( $2\theta = 38.2^\circ$ ) could be observed, indicating that the Au species had aggregated to form metallic Au crystallite. The fact that there was also no detectable crystallite of Au species over 2.9 wt% Au/Fe-C2 indicated that only when calcined at temperature higher than 200 °C gold nano-particles would aggregated remarkably.

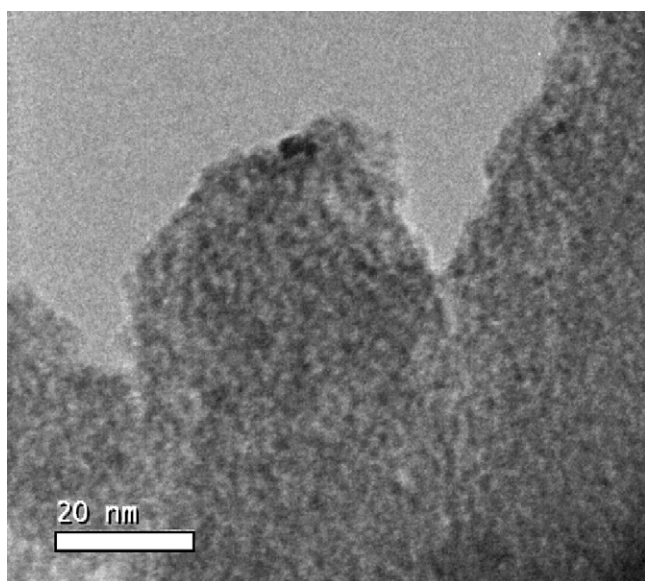
HRTEM observations of the 2.5 wt% Au/Fe-UC, 2.9 wt% Au/Fe-C2 and 3.3 wt% Au/Fe-C4 were shown in Figs. 9–11. It could be seen that, over 2.5 wt% Au/Fe-UC catalyst, Au was highly dispersed that no Au nano-particles could be observed, Fig. 9. This suggests that Au is either atomically dispersed, or else is in a sub-nanometer particle form that is impossible to distinguish from the speckle contrast exhibited by the support. Furthermore, the support seemed more uniform and amorphous, which was considered to be important to have the uniformly distributed nano-sized Au metal [27]. After being calcined at 200 °C, Au was also highly dispersed and there were also almost no Au nano-particles that could be observed, indicating that Au was highly dispersed even after being calcined at 200 °C. The supports aggregated and many small particles with diameters of 3–5 nm distributed uniformly, Fig. 10(a). In addition, over Au/Fe-C2 catalyst, crystal of ferric oxide could also be observed occasionally (the crystal lattice of 0.25 nm corresponding to  $\text{Fe}_2\text{O}_3$  (1 1 0) crystal surface), Fig. 10(b), suggesting the transformation from ferric hydroxide to ferric oxide had began at this temperature. As for Au/Fe-C4 catalyst, a dispersion of discrete metallic Au nano-particles with typical

Table 1  
Some physicochemical properties of the supported Au catalysts

	Au loading (wt%)	BET surface area ( $\text{m}^2/\text{g}$ )	Average pore diameter (Å)	B.E. of Au 4f (eV)	B.E. of Fe 2p (eV)	B.E. of O 1s (eV)	B.E. of N 1s (eV)	Area ratio of $\text{Au}^+/\text{Au}^0$
Au/Fe-UC	2.5	328.4	22.1	84.2, 87.7	711.6	530.9	400.0	0.65
Au/Fe-C2	2.9	194.7	39.0	84.2, 87.9	711.2	530.2	–	0.33
Au/Fe-C4	3.3	20.13	106.6	83.8	711.0	530.1	–	0



**Fig. 8.** XRD patterns of different supported Au catalysts, (a) 2.5 wt% Au/Fe-UC, (b) 2.9 wt% Au/Fe-C2 and (c) 3.3 wt% Au/Fe-C4.



**Fig. 9.** HRTEM pictures of catalysts 2.5 wt% Au/Fe-UC.

diameters of 2–4 nm is clearly visible, Fig. 11. They are supported on highly crystalline  $\alpha$ -Fe<sub>2</sub>O<sub>3</sub> grains which are typically about 30 nm in size. Such an observation correlates well with the

measured drop of surface area from 328.4 m<sup>2</sup> g<sup>-1</sup> in the uncalcined state to 20.1 m<sup>2</sup> g<sup>-1</sup> in the calcined state.

Results of FT-IR measurements for 2.5 wt% Au/Fe-UC, 2.9 wt% Au/Fe-C2 and 3.3 wt% Au/Fe-C4 are shown in Fig. 12. The Au/Fe-UC catalysts exhibited broad and strong absorbance at 2800–3680 cm<sup>-1</sup> and this absorbance can be attributed to the stretching vibration of OH group which was mainly contributed by the supports of Fe(OH)<sub>x</sub> and adsorbed water. In addition, three intensive bands in the 1280–1780 cm<sup>-1</sup> region were observed in the spectra of 2.5 wt% Au/Fe-UC catalyst. The band centered at about 1630 cm<sup>-1</sup> can be attributed to the deformation vibration of OH. The other two intensive bands centered at 1494 and 1353 cm<sup>-1</sup> may be due to superposition of carbonate and nitrate species on the iron support [28,29]. Calcination at 200 °C resulted in the removal of physisorbed water because of the significant decrease of the intensity of the absorbance bands at 1630 cm<sup>-1</sup> and in the region of 2800–3680 cm<sup>-1</sup>. Calcination at 200 °C also made the carbonate and nitrate species on the iron support decompose confirmed by the complete disappearance of 1494 and 1353 cm<sup>-1</sup> bands. Calcination at 400 °C resulted in the supports' transformation from Fe(OH)<sub>x</sub> to Fe<sub>2</sub>O<sub>3</sub> according to the almost complete disappearance of 1630 cm<sup>-1</sup> bands and the absorbance in the 2800–3680 cm<sup>-1</sup> region.

In order to get further insight into the fact that the uncalcined catalysts had the higher activity, computer simulation of O<sub>2</sub> adsorption on Au (1 0 0) was performed with DMol<sup>3</sup>/Materials Studio (Accelrys). After being optimized, the one which has the lowest energy among four possible models was chosen as the standard for investigation. When adsorbed on Au (1 0 0) crystal cell surface, the bond distance of O–O (1.444 Å) was much longer than the standard bond distance of O<sub>2</sub> (1.225 Å), indicating that the adsorbed O<sub>2</sub> had been activated. The calculating results show that adsorption of O<sub>2</sub> on Au (1 0 0) crystal surface was an exothermic reaction with the adsorption heat of –78.57 kJ/mol. For compare purpose, adsorption of O<sub>2</sub> on Au crystal cell with one positive electric charge was also investigated, and the bond distance of O–O was changed to 1.427 Å, only slightly shortened. Also, the bond distance of Au–O changed unremarkably. However, the adsorption heat was decreased severely from –78.57 kJ/mol to –401.01 kJ/mol, indicating that adsorption of O<sub>2</sub> on Au<sup>+</sup> was a strong exothermic reaction and O<sub>2</sub> was more easily adsorbed on Au<sup>+</sup>. In addition, the distributing of electric charge when O<sub>2</sub> adsorbed on Au (1 0 0) crystal surface without electric charge or taking one positive electric charge were investigated. On Au crystal cell without electric charge, the O

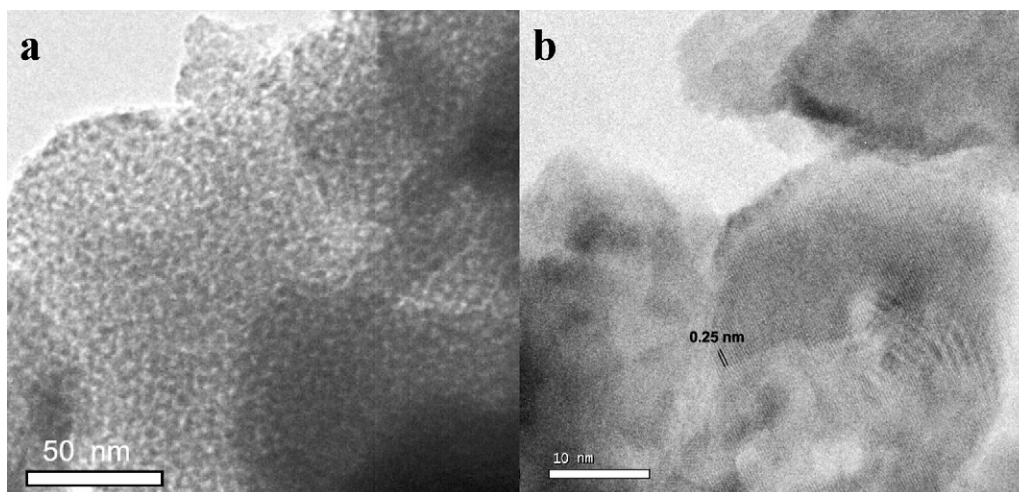


**Fig. 10.** HRTEM pictures of catalysts 2.9 wt% Au/Fe-C2.

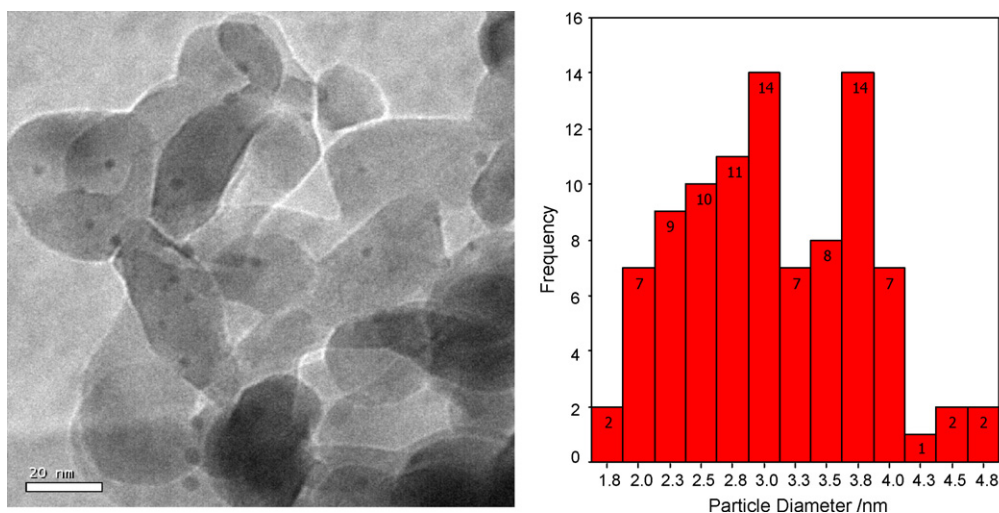


Fig. 11. HRTEM picture and particles distribution of catalysts 3.3 wt% Au/Fe-C4.

atom takes  $-0.270$  negative electric charge, while the conjoint Au atom takes  $0.140$  or  $0.150$  positive electric charge. Based on the Coulomb's law:  $f = q^+q^-/r^2$ , the electrostatic gravitation between Au and O atom on  $Au^+$  was stronger than that on  $Au^0$ , indicating that Au taking positive electric charge was in favor of the adsorption and activation of  $O_2$  and consequently could promote the subsequent oxidation reactions. Furthermore, two models of  $O_2$  adsorbed on Au crystal cell taking two and three positive electric charges were also investigated (not shown here). The bond distance of O–O were  $1.422 \text{ \AA}$  and  $1.379 \text{ \AA}$ , respectively, slightly decreased with increase of electric charge and the corresponding adsorption heat were  $-683.49 \text{ kJ/mol}$  and  $-992.17 \text{ kJ/mol}$ , respectively, indicating that Au crystal cell taking more positive electric charge were more favorable for the adsorption of  $O_2$ .

Also, four possible models of CO adsorption on Au (100) surface were designed and optimized. It was found that the

adsorption heat of CO was  $34.16 \text{ kJ/mol}$ , greatly higher than that of  $O_2$ , indicating that the adsorption of CO on Au (100) surface was an endothermic reaction. So the models of CO adsorption were not discussed here.

#### 4. Discussion

It is apparent from the characterization that the uncalcined catalysts are very different from the corresponding catalysts calcined at  $200 \text{ }^\circ\text{C}$  and  $400 \text{ }^\circ\text{C}$ . The uncalcined catalysts consist of amorphous ferric hydroxide on which the Au is uniformly dispersed into sub-nano-particles in the form of coexistence of  $Au^+$  and  $Au^0$ . When calcined at  $200 \text{ }^\circ\text{C}$ , the supports would aggregate to disordered agglomerates of  $3\text{--}5 \text{ nm}$  ferric hydroxide particles on which Au is still uniformly dispersed in the form of coexistence of  $Au^+$  and  $Au^0$ . While after being calcined at  $400 \text{ }^\circ\text{C}$ , the catalysts are comprised of  $2\text{--}4 \text{ nm}$  metallic Au particles

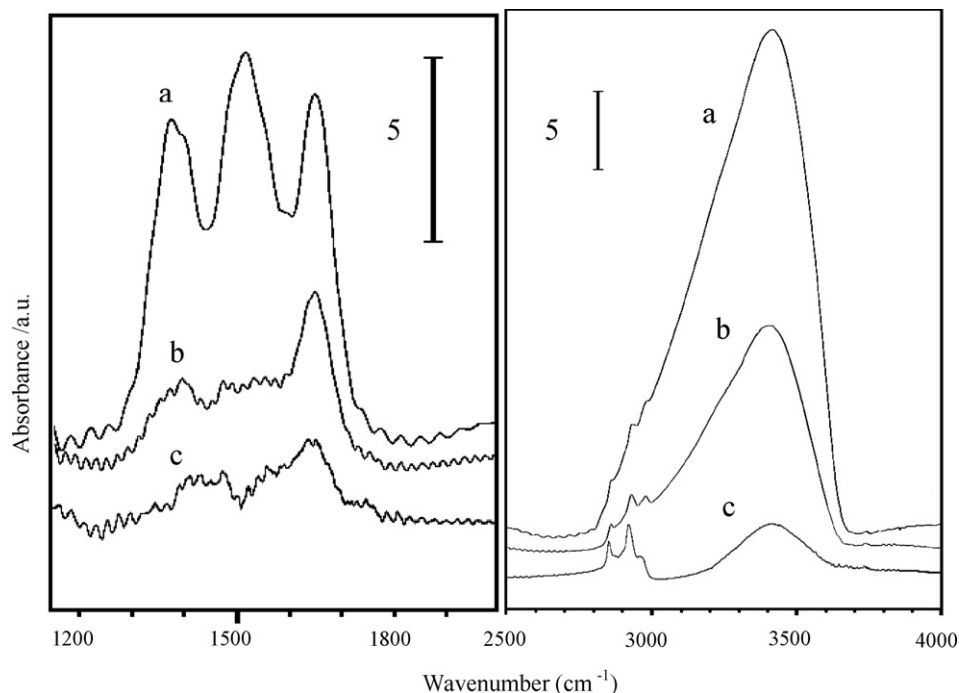


Fig. 12. FT-IR spectra of different supported Au catalysts, (a) 2.5 wt% Au/Fe-UC, (b) 2.9 wt% Au/Fe-C2 and (c) 3.3 wt% Au/Fe-C4.

supported on well-crystalline  $\alpha$ -Fe<sub>2</sub>O<sub>3</sub> particles with 30 nm diameter. In addition, the uncalcined catalysts contain some carbonate and nitrate species and even some water.

In our work, the computer simulations showed that Au atom cluster could adsorb O<sub>2</sub> and activate it. It is generally regarded that the adsorption of O<sub>2</sub> on Au is very weak, so that much attention was paid to the study of CO adsorption on Au [30–33]. While Kim et al. found that the formation of the activated di-oxygen species was the key for the unusual catalytic activities of Au-based catalysts [34]. Some papers also studied the adsorption of O<sub>2</sub> on Au and found that the O<sub>2</sub> adsorption energy showed odd-even effects [35,36]. Recently, Mullins and co-workers provided the evidence for the presence of O<sub>2</sub> on Au(1 1 1) and on Au clusters supported on a TiO<sub>2</sub>(1 1 0) surface following exposure of these samples to a plasma-jet source of oxygen [37]. Our simulations results showed that the O<sub>2</sub> adsorption energy was more lower than the CO adsorption energy, indicating the key of the CO oxidation was the activation of O<sub>2</sub> on Au. The model also showed that Au takes positive charge could more easily adsorb O<sub>2</sub> and it could illustrate the fact that Au<sup>+</sup> or Au<sup>3+</sup> is higher active than Au<sup>0</sup>, which has been widely proved recently [38–40].

For H<sub>2</sub> oxidations, supported Au catalysts are not very effective as compared with traditional supported Pd and Pt catalysts. While in this work, it was found that H<sub>2</sub> oxidations were less sensitive to the calcinations temperatures. Considering the characterization results, it can be conjectured that H<sub>2</sub> oxidations were less sensitive to the size of nano Au particles and the chemistry state of Au, that is, the activities of supported Au catalysts with Au<sup>+</sup> or Au<sup>0</sup> and with large or small Au particles are nearly same.

When tested for CO oxidation and CO selective oxidations in the presence of H<sub>2</sub>, both activity and selectivity decreased with the increase of the calcination temperatures. Considering that the activity of the three catalysts for H<sub>2</sub> oxidation is close, so the decrease of selectivity is due to the decrease of the activity for CO oxidations. At first sight, the catalysts calcined at 400 °C should accord the conventional wisdom that 2–5 nm supported Au particles on a metal-oxide support are beneficial because of the optimized length of interfacial perimeter that they expose. While, when the Bond and Thompson models is considered [39], less activity will be related to the fact that: (i) the requisite mixture of Au<sup>0</sup> and Au<sup>+</sup> species is absent, and (ii) the oxide support may be too perfect leading to a deficiency in active superoxide species. By contraries, the uncalcined catalysts possessing higher activity may be related to the following reason. Firstly, the uncalcined catalysts contain the active species Au<sup>+</sup>/Au<sup>0</sup> and the supports contain large amount of OH groups, which was regarded to be very important for CO oxidation. According to Kung's reports [41], the hydroxyl group is associated with Au<sup>+</sup> and active site is an ensemble of Au<sup>+</sup>-OH<sup>-</sup> together with Au<sup>0</sup> atoms. The Au<sup>+</sup> with a hydroxyl ligand provides the pathway for the conversion of CO to CO<sub>2</sub>. In our work, the catalysts were dried for several hours at 100 °C and the catalytic activity for CO oxidations was almost not decreased, indicating the OH group associated with Au<sup>+</sup> was mostly provided by the support of Fe(OH)<sub>x</sub>. Secondly, recently Xu and co-workers found that the catalytic activity of Au nano-particles in Au/ZrO<sub>2</sub> for CO oxidation can be greatly improved by reducing the particle size of zirconia nano-particles [42]. In particular, the catalysts consisting of comparably sized Au-metal (4–5 nm) and ZrO<sub>2</sub> (5–15 nm) nano-particles are advantageous over those containing similarly sized Au metal but larger ZrO<sub>2</sub> particles. This indicates that, if the size of particles of active noble metal is close to that of the particles of the supports, the catalysts would have a higher activity for CO oxidations. Such case may also occur in our work that, over uncalcined catalysts, the fact that the Au species are uniformly dispersed into the uniformly dispersed supports result in a higher

activity. While over catalysts calcined at 400 °C, both the supports and the Au species aggregated and this resulted in the case that the Au particles do not match the support particles. Thirdly, the uncalcined catalysts contained some nitrates, and this may be a reason that the uncalcined catalysts have higher activity, since Hutchings and co-workers found recently that nitrates had promotional effect on the supported Au catalysts for CO oxidation [25]. Lastly, the larger BET surface may be another important reason for the higher activity considering the uncalcined catalyst are 10 times larger than that of the catalysts calcined at 400 °C.

Compared with calcined catalysts, the uncalcined catalysts also have an advantage in the preparation process. As mentioned in the end of Section 1, in the calcination process, some nitrate and carbonate would be decomposed and environment pollution gas such as NO<sub>x</sub>, HCl, and CO<sub>2</sub>, etc., would be emitted. In addition, calcinations at elevated temperature is a energy exhausting process. Preparing uncalcined catalysts could omit this preparation step, therefore, it is, relatively, an environment friendly process.

## 5. Conclusion

In conclusion, a new ferric hydroxide supported gold catalyst prepared with co-precipitation method at room temperature without any heat treatment exhibited high catalytic activity and high selectivity for CO oxidation in air and for CO selective oxidation in the presence of H<sub>2</sub>, providing the example of CO complete oxidation with selectivity approaching to 100% below or at room temperature. The results of activity measurement show that the activity and CO selectivity of this catalyst would decrease when it was calcined at elevated temperatures, such as 200 and 400 °C. The results also show that the temperature for selective CO oxidation in the presence of H<sub>2</sub> could be set by adjusting gold loadings without decreasing the CO selectivity and CO over this catalyst had a good ability of competitive consuming of O<sub>2</sub> even at 200 °C and in excessive H<sub>2</sub>. XPS and CS results indicate that Au<sup>+</sup> in the catalysts has a positive effect on CO oxidations. XRD and HRTEM show that small Au particles are in a sub-nano level and are very active for CO oxidations. FT-IR indicate that uncalcined catalysts contain lots of OH group and some nitrate and this would be favorable for the higher activity. In addition, the preparing process of this catalyst is not only simple, but also relatively environment friendly, and such a process may be expanded to the preparations of other supported noble metal catalyst, such as Pd or Pt, etc.

## Acknowledgements

The Authors would like to thank Ms. L. Gao for the XPS investigation, Ms. Q. Wu for the gold loading analysis, Ms. L. He for the XRD investigation, Ms. J. Li for the measurement of BET adsorption. We also thank Mr. J.M. Chen for the observation of HRTEM picture and thank Mr. Y. Wang for the help of computer simulations.

## References

- [1] M.J. Kahlich, H.A. Gasteiger, R.J. Behm, J. Catal. 171 (1997) 93–105.
- [2] G.W. Xu, Z.G. Zhang, J. Power Sources 157 (2006) 64–67.
- [3] H. Tanaka, S.I. Ito, S. Kameoka, K. Tomishige, K. Kunimori, Catal. Comm. 4 (2003) 1–4.
- [4] A. Manasilp, E. Gulari, Appl. Catal. B 37 (2002) 17–25.
- [5] M. Watanabe, H. Uchida, K. Okhubo, H. Igarashi, Appl. Catal. B 46 (2003) 595–600.
- [6] Y. Minemura, S. Ito, T. Miyao, S. Naito, K. Keichi, K. Kunimori, Chem. Comm. 11 (2005) 1429–1431.
- [7] E.Y. Ko, E.D. Park, H.C. Lee, D. Lee, S. Kim, Angew. Chem. Int. Et. 46 (2007) 734–737.
- [8] K.I. Tanaka, Y. Moro-okab, K. Ishigurea, T. Yajimaa, Y. Okabe, Y. Kato, H. Hamano, S. Sekiya, H. Tanaka, Y. Matsumoto, H. Koinuma, H. He, C. Zhang, Q. Feng, Appl. Catal. A 92 (2006) 115–121.

- [9] K.I. Tanaka, a.M. Shou, H. He, X. Shi, *Appl. Catal. A* 110 (2006) 185–190.
- [10] M. Haruta, S. Tsubota, T. Kobayashi, H. Kageyama, M. Genet, B. Delmon, *J. Catal.* 144 (1993) 175–192.
- [11] M. Haruta, N. Yamada, T. Kobayashi, S. Iijima, *J. Catal.* 115 (1989) 301–309.
- [12] M. Okumura, S. Nakamura, S. Tsubota, T. Nakamura, M. Azuma, M. Haruta, *Catal. Lett.* 51 (1998) 53–58.
- [13] S. Minico, S. Scire, C. Crisafulli, S. Gavagno, *Appl. Catal. B* 34 (2001) 277–285.
- [14] M. Haruta, T. Kobayashi, H. Sano, N. Yamada, *Chem. Lett.* (1987) 405–408.
- [15] R.M. Torres Sanchez, A. Ueda, K. Tanaka, M. Haruta, *J. Catal.* 168 (1997) 125–127.
- [16] G.K. Bethke, H.H. Kung, *Appl. Catal. A* 194/195 (2000) 43–53.
- [17] R.J.H. Grisel, B.E. Nieuwenhuys, *J. Catal.* 199 (2001) 48–59.
- [18] R.J.H. Grisel, C.J. Weststrate, A. Goossens, M.W.J. Crajé, A.M. van der Kraan, B.E. Nieuwenhuys, *Catal. Today* 72 (2002) 123–132.
- [19] W.Y. Yu, C.P. Yang, J.N. Lin, C.N. Kuo, B.Z. Wan, *Chem. Comm.* 3 (2005) 354–356.
- [20] M. Lomello-Tafin, A.A. Chaou, F. Morfin, V. Caps, J.L. Rousset, *Chem. Comm.* 3 (2005) 388–390.
- [21] S. Carrettin, P. Concepcion, A. Corma, J.M.L. Nieto, V.F. Puentes, *Angew. Chem. Int. Ed.* 43 (2004) 2538.
- [22] M.M. Schubert, A. Venugopal, M.J. Kahlich, V. Plzak, R.J. Behm, *J. Catal.* 222 (2004) 32–40.
- [23] P. Landon, J. Ferguson, B.E. Solsona, T. Garcia, A.F. Carley, A.A. Herzing, C.J. Kiely, S.E. Golunski, G.J. Hutchings, *Chem. Comm.* 27 (2005) 3385–3387.
- [24] B.T. Qiao, Y.Q. Deng, *Chem. Comm.* 17 (2003) 2192–2193.
- [25] B. Solsona, M. Conte, Y. Cong, A. Carley, G.J. Hutchings, *Chem. Comm.* 18 (2005) 2351–2353.
- [26] N.A. Hodge, C.J. Kiely, R. Whyman, M.R.H. Siddiqui, G.J. Hutchings, Q.A. Pankhurst, F.E. Wagner, R.R. Rajaram, S.E. Golunski, *Catal. Today* 72 (2002) 133–144.
- [27] K.C. Wu, Y.L. Tung, Y.L. Chen, Y.W. Chen, *Appl. Catal. B* 53 (2004) 111–116.
- [28] A.P. Kozlova, S. Sugiyama, A.I. Kozlov, K. Asakura, Y. Iwasawa, *J. Catal.* 176 (1998) 426–438.
- [29] A.P. Kozlova, A.I. Kozlov, S. Sugiyama, Y. Matsui, K. Asakura, Y. Iwasawa, *J. Catal.* 181 (1999) 37–48.
- [30] D.C. Meier, D.W. Goodman, *J. Am. Chem. Soc.* 126 (2004) 1892–1899.
- [31] S. Derrouiche, P. Gravejat, D. Bianchi, *J. Am. Chem. Soc.* 126 (2004) 13010–13015.
- [32] S.T. Daniells, A.R. Overweg, M. Makkee, J.A. Moulijn, *J. Catal.* 230 (2005) 52–65.
- [33] G. Smit, N. Strukan, M.W.J. Craje, K. Lazar, *J. Mol. Catal. A* 252 (2006) 163–170.
- [34] Y.D. Kim, M. Fischer, G. Gantefer, *Chem. Phys. Lett.* 377 (2003) 170–176.
- [35] A. Franceschetti, S.J. Pennycook, S.T. Pantelides, *Chem. Phys. Lett.* 374 (2003) 471–475.
- [36] E.M. Fernandez, P. Ordejon, L.C. Balbas, *Chem. Phys. Lett.* 408 (2005) 252–257.
- [37] J.D. Stiehl, T.S. Kim, S.M. McClure, C.B. Mullins, *J. Am. Chem. Soc.* 126 (2004) 1606–1607.
- [38] G.C. Bond, D.T. Thompson, *Gold Bull.* 33 (2000) 41.
- [39] J. Guzman, B.C. Gates, *J. Am. Chem. Soc.* 126 (2004) 2672–2673.
- [40] G.J. Hutchings, M.S. Hal, A.F. Carle, P. Landon, B.E. Solsona, C.J. Kiely, A. Herzing, M. Makkee, J.A. Moulijn, A. Overweg, J.C. Fierro-Gonzalez, J. Guzman, B.C. Gates, *J. Catal.* 242 (2006) 71–81.
- [41] C.H. Costello, M.C. Kung, H.S. Oh, Y. Wang, H.H. Kung, *Appl. Catal. A* 232 (2002) 159–168.
- [42] X. Zhang, H. Wang, B.Q. Xu, *J. Phys. Chem. B* 109 (2005) 9678–9683.